

## The Chemistry of Niobium and Tantalum Dithiocarbamate-complexes. Part 5.<sup>1</sup> The Kinetics and Mechanism of the Hydrazine-forming Reactions between [ $\{M(S_2CNEt_2)_3\}_2(\mu-N_2)$ ] ( $M = Nb$ or $Ta$ ) and Acid: Rate-limiting Protonation

Richard A. Henderson,\* Susan H. Morgan, and Alan N. Stephens

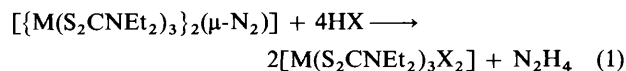
AFRC Institute of Plant Science Research, Nitrogen Fixation Laboratory, University of Sussex, Brighton BN1 9RQ

The kinetics of the reactions between [ $\{M(S_2CNEt_2)_3\}_2(\mu-N_2)$ ] and HX ( $M = Nb$ ,  $X = Cl$  or  $Br$ ;  $M = Ta$ ,  $X = Cl$ ) to yield [ $M(S_2CNEt_2)_3X_2$ ] and hydrazine have been studied in MeCN at 25.0 °C. In all cases the multistep mechanism involves rate-limiting protonation of the bridging dinitrogen atoms, and in one case ( $M = Ta$ ) the monoprotonated species [ $\{Ta(S_2CNEt_2)_3\}_2(\mu-N_2H)^+$ ] was detected spectrophotometrically. The cleavage of the metal–nitrogen bond occurs after the addition of at least two protons. The factors influencing the rates of protonation of bridging and end-on co-ordinated dinitrogen molecules are discussed.

Over the last two decades detailed studies have established how a mononuclear, end-on co-ordinated dinitrogen molecule can be converted into ammonia or hydrazine by a sequence of simple electron- and proton-transfer reactions.<sup>2</sup> In contrast, relatively little is known of how bridging dinitrogen ligands are activated towards protic attack. Such information is crucial to our goal of understanding how the enzyme nitrogenase operates at the atomic level. We still have relatively little information about the geometry of the active site in this enzyme, and binuclear or even polynuclear interactions between metals and the substrate remain a distinct possibility.

On the basis of kinetic analyses, polynuclear structures for the reduction of dinitrogen have been proposed in several chemical systems, most notably those based on vanadium and titanium.<sup>3,4</sup> However these systems are not ideally suited for a detailed mechanistic interpretation since the reactions involve a large number of steps, in some cases the structures of neither the reactants nor the products are known, and in others the molecule contains both bridging and end-on dinitrogen ligands.<sup>4</sup> The development of the chemistry based on the ' $M(S_2CNEt_2)_3$ ' core has permitted mechanistic studies on the protonation of bridging dinitrogen complexes free from many of these restrictions.

The system shown in equation (1) ( $M = Nb$  or  $Ta$ ,  $X = Cl$  or



$Br$ ) has the major advantages that it is stoichiometric, that examples of the reactants and products have been structurally characterised by X-ray crystallography,<sup>5</sup> that it contains only one type of dinitrogen ligand, and that it is soluble in MeCN, thus allowing a detailed quantitative analysis of the kinetics.<sup>6</sup>

In this paper we describe the kinetics for the systems [ $\{Nb(S_2CNEt_2)_3\}_2(\mu-N_2)$ ] with HCl or HBr and [ $\{Ta(S_2CNEt_2)_3\}_2(\mu-N_2)$ ] with HCl, all of which exhibit rate-limiting protonation of the bridging dinitrogen ligand. In the following paper we shall discuss the kinetics of the reaction between [ $\{Ta(S_2CNEt_2)_3\}_2(\mu-N_2)$ ] and HBr which shows a very different pattern. Together the two papers allow a comprehensive mechanism to be defined for the protonation of these dinitrogen complexes.

### Experimental

All manipulations were routinely performed under an atmosphere of dinitrogen using standard Schlenk and syringe techniques.

The dinitrogen complexes [ $\{M(S_2CNEt_2)_3\}_2(\mu-N_2)$ ] ( $M = Nb$  or  $Ta$ ) were prepared as described before,<sup>5</sup> and gave satisfactory microanalytical results and <sup>1</sup>H n.m.r. spectra. Acetonitrile was freshly distilled from CaH<sub>2</sub> immediately prior to use, and solutions of anhydrous HCl<sup>7</sup> and HBr<sup>8</sup> were prepared as described before.

*Kinetic Studies.*—All kinetic studies were performed on an Aminco-Morrow stopped-flow apparatus, modified for use with air-sensitive solutions, and interfaced to a B.B.C. micro-computer, *etc.*, as described before.<sup>8</sup>

Analysis of the results was by the necessary straight-line graphs (see below) and errors on the slopes and intercepts of such graphs were established by a linear least-squares analysis.

### Results and Discussion

The results we shall discuss herein are on the kinetic studies of [ $\{Ta(S_2CNEt_2)_3\}_2(\mu-N_2)$ ] with HCl and [ $\{Nb(S_2CNEt_2)_3\}_2(\mu-N_2)$ ] with HCl or HBr in MeCN. The mechanistic conclusions from these three studies are similar: that the rate-limiting step in the hydrazine-forming reactions is protonation of the bridging nitrogen atoms. However the very different nature of the acid–base couples studied means that the kinetics associated with the three systems are very different.

*Reaction of [ $\{Ta(S_2CNEt_2)_3\}_2(\mu-N_2)$ ] with HCl.*—The reaction of [ $\{Ta(S_2CNEt_2)_3\}_2(\mu-N_2)$ ] with an excess of HCl in MeCN occurs in two phases, as shown by the absorbance–time traces shown in Figure 1. Thus at  $\lambda = 400$  nm an initial rise in absorbance is followed by a decrease to yield the products. Both phases are exponential and the dependence of the slower phase on the concentration of HCl was established at  $\lambda = 450$  nm (Figure 1, main) where the absorbance change associated with the fast phase was negligible. The kinetics of the slow phase exhibited a first-order dependence on the concentrations of both the dinitrogen complex and HCl, as shown in Figure 2, and described by equation (2), where  $a = (4.5 \pm 0.1) \times 10^3 \text{ dm}^3$

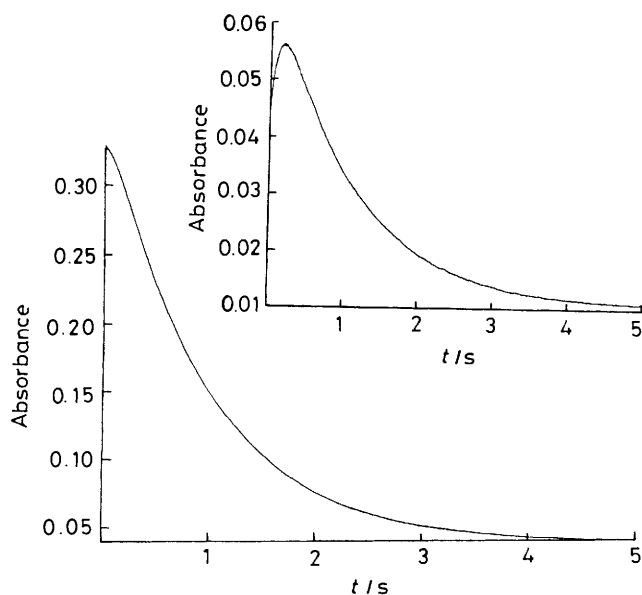


**Figure 1.** Absorbance-time trace observed at  $\lambda = 450$  nm for the reaction of  $[\{\text{Ta}(\text{S}_2\text{CNET}_2)_3\}_2(\mu\text{-N}_2)]$  with HCl in MeCN at 25.0 °C. Insert: same reaction monitored at  $\lambda = 400$  nm. Concentration of  $[\{\text{Ta}(\text{S}_2\text{CNET}_2)_3\}_2(\mu\text{-N}_2)] = 5 \times 10^{-5}$  mol dm $^{-3}$  and concentration of HCl = 1.0 mmol dm $^{-3}$ .

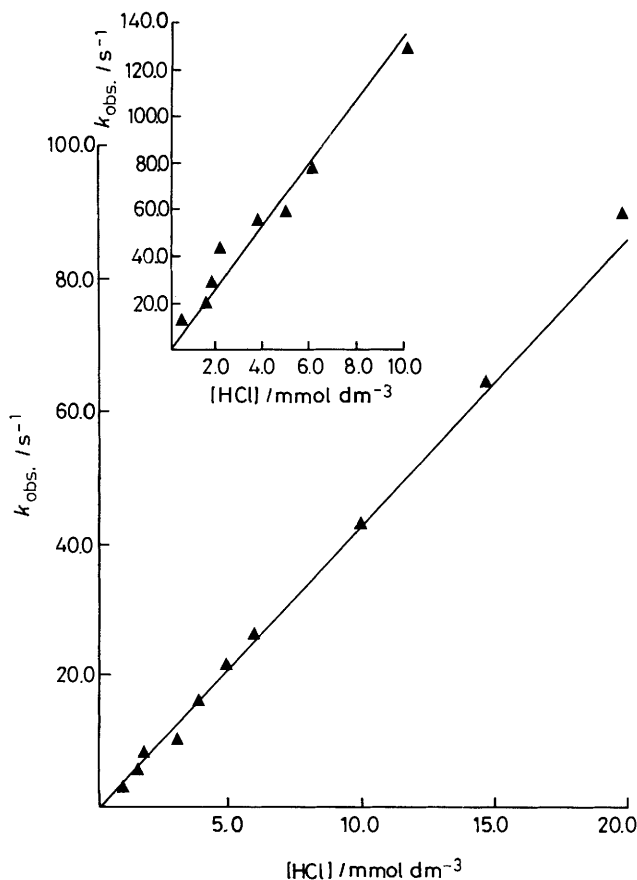
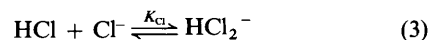


**Figure 2.** Dependence of  $k_{\text{obs}}$  on the concentration of HCl for the reaction between  $[\{\text{Ta}(\text{S}_2\text{CNET}_2)_3\}_2(\mu\text{-N}_2)]$  and HCl in MeCN at 25.0 °C, showing the data for the slow phase and (insert) the fast phase

$$k_{\text{obs}} = a[\text{HCl}] \quad (2)$$

mol $^{-1}$  s $^{-1}$ . Here and throughout this paper,  $k_{\text{obs}}$  is the measured first-order rate constant observed under conditions where the acid is in a large excess over the concentration of dimer. Furthermore the concentration of acid is that calculated having allowed for the homoconjugation and acid-base equilibria shown in equations (3) and (4) respectively, using the literature



values<sup>6</sup> of  $K_{\text{Cl}} = 1.58 \times 10^2$  dm $^3$  mol $^{-1}$  and  $K_a = 1.26 \times 10^{-9}$ .

Using the derived values for the observed rate constants for the slow phase, the kinetics of the fast phase were established by an exponential curve-fitting procedure to the traces observed at  $\lambda = 400$  nm. In this manner the kinetics of the first phase was shown to be first order in the concentrations of both the dinitrogen complex and HCl as shown in Figure 2 (insert) and described by equation (2),  $a = (1.3 \pm 0.1) \times 10^4$  dm $^3$  mol $^{-1}$  s $^{-1}$ . Kinetic data for the reactions of HCl with  $[\{\text{Ta}(\text{S}_2\text{CNET}_2)_3\}_2(\mu\text{-N}_2)]$  are collected in Table 1.

Before we can interpret the biphasic behaviour shown in Figure 1 it is important to appreciate that for consecutive reactions of this type two mathematical solutions exist,<sup>9</sup> and the behaviour shown at  $\lambda = 450$  nm does not dictate a fast initial phase and a slow second phase. There is no general method for solving this dichotomy, particularly when both phases exhibit identical kinetics, as in the present case. However we have developed an analysis for this system which not only defines which phase comes first but also establishes the stoichiometry of the spectrophotometrically detected intermediate.

In the presence of an excess of HCl and  $[\text{NET}_4]\text{Cl}$  the reaction with  $[\{\text{Ta}(\text{S}_2\text{CNET}_2)_3\}_2(\mu\text{-N}_2)]$  exhibits a single exponential absorbance-time trace at all wavelengths. The kinetic data observed under these conditions are shown in Table 1. The analysis of the dependence of the reaction rate on the concentrations of HCl and  $\text{Cl}^-$  is complicated in aprotic solvents by the homoconjugation and acid-base equilibria shown in equations (3) and (4), respectively. Using the literature values of  $K_{\text{Cl}}$  and  $K_a$  the values of  $[\text{HCl}]$  and  $[\text{Cl}^-]$  were calculated at equilibrium, and the dependence of  $k_{\text{obs}}$  on  $[\text{HCl}]/[\text{Cl}^-]$  is shown in Figure 3, from which the empirical rate equation (5) was derived. This rate equation is consistent

$$k_{\text{obs}} = \frac{(1.0 \pm 0.2) \times 10^3 [\text{HCl}]^2}{[\text{Cl}^-] + (0.25 \pm 0.02)[\text{HCl}]} \quad (5)$$

with the sequence of protonation steps shown in the Scheme. If we treat the monoprotonated species,  $[\{\text{M}(\text{S}_2\text{CNET}_2)_3\}_2(\mu\text{-N}_2\text{H})]^+$  (B), as a steady-state intermediate then the rate equation (6) can be derived, which by comparison with (5) allows the determination of the values  $k_1 = (4.0 \pm 0.2) \times 10^3$  dm $^3$  mol $^{-1}$  s $^{-1}$  and  $k_2/k_{-1} = 0.25 \pm 0.02$ . The most important feature of equation (6) is that it defines unambiguously the rate

$$k_{\text{obs}} = \frac{k_1 k_2 [\text{HCl}]^2}{k_{-1} [\text{Cl}^-] + k_2 [\text{HCl}]} \quad (6)$$

constant for the initial protonation step. The derived value of  $k_1$  is in excellent agreement with the rate constant measured for the slow phase in the studies performed in the absence of  $[\text{NET}_4]\text{Cl}$ . Using the now established value for  $k_2 = (1.3 \pm 0.1) \times 10^4$  dm $^3$  mol $^{-1}$  s $^{-1}$  (determined from the fast phase in the studies in the absence of  $[\text{NET}_4]\text{Cl}$ ) the value of  $k_{-1} = (5.2 \pm 0.1) \times 10^4$

**Table 1.** Kinetic data for the reaction between  $[\{\text{Ta}(\text{S}_2\text{CNEt}_2)_3\}_2(\mu\text{-N}_2)]$  ( $2.5 \times 10^{-5} \text{ mol dm}^{-3}$ ) and HCl in MeCN ( $25.0^\circ\text{C}$ ,  $\lambda = 400$  or  $450 \text{ nm}$ )

[HCl] <sup>a</sup> / mmol dm <sup>-3</sup>	[Cl <sup>-</sup> ] <sup>a,b</sup> / mmol dm <sup>-3</sup>	$k_{\text{obs.}}^c/\text{s}^{-1}$	
		fast	slow
1.0		13.0(10.0)	3.0(2.5)
1.5		20.2	6.0(5.5)
2.0		28.0(20.0)	8.3
3.0		45.0(26.0)	10.2
4.0		55.2	16.1
5.0		60.3(45.3)	22.4
5.0 <sup>d</sup>		61.0	21.6
5.0 <sup>e</sup>		60.5	21.9
6.0		80.4	26.0(20.5)
10.0		130.0(97.0)	43.2(25.0)
15.0		(144.0)	64.0(53.0)
20.0			90.0(71.3)
2.0	1.0		3.6 <sup>f</sup>
	2.0		1.4
	4.0		0.8
10.0	1.0		27.0
	2.0		23.0
	4.0		15.6
	5.0		13.0
	6.0		9.7
20.0	1.0		85.0
	2.0		75.0
	4.0		65.0
	5.0		55.0
	6.0		50.0
	8.0		36.0
2.5	1.0		3.6
5.0			11.8
10.0			27.0
15.0			56.8
20.0			80.3
5.0	4.0		3.3
10.0			19.0
15.0			46.2
20.0			76.3

<sup>a</sup> Concentrations of HCl and Cl<sup>-</sup> shown are those added to the reaction mixture. The concentrations shown in the Figures are those corrected for the homoconjugation and acid-base equilibria of equations (3) and (4). <sup>b</sup> Chloride supplied as [NEt<sub>4</sub>]Cl. <sup>c</sup> Values shown in parentheses are the rate constants measured using DCl. <sup>d</sup>  $5.0 \times 10^{-5} \text{ mol dm}^{-3}$  [ $\{\text{Ta}(\text{S}_2\text{CNEt}_2)_3\}_2(\mu\text{-N}_2)$ ]. <sup>e</sup>  $1.25 \times 10^{-5} \text{ mol dm}^{-3}$  [ $\{\text{Ta}(\text{S}_2\text{CNEt}_2)_3\}_2(\mu\text{-N}_2)$ ]. <sup>f</sup> Only single phase observed in the studies with [NEt<sub>4</sub>]Cl.

$\text{dm}^3 \text{ mol}^{-1} \text{ s}^{-1}$  can be calculated. These elementary rate constants are collected in Table 3, and we shall return a little later to a discussion of the rates of these protonation reactions. Having established the correct rate constants for  $k_1$  and  $k_2$  the true visible absorption spectrum of  $[\{\text{Ta}(\text{S}_2\text{CNEt}_2)_3\}_2(\mu\text{-N}_2\text{H})]^+$  was calculated<sup>9</sup> as shown in Figure 4.

The monophasic absorbance-time traces observed in the presence of [NEt<sub>4</sub>]Cl for the reaction between  $[\{\text{Ta}(\text{S}_2\text{CNEt}_2)_3\}_2(\mu\text{-N}_2)]$  and HCl on the one hand, and the biphasic traces observed in the presence of HCl alone on the other, are a consequence of the large excess of chloride present in the former studies. The presence of this strong base has the effect of rapidly deprotonating the  $[\{\text{Ta}(\text{S}_2\text{CNEt}_2)_3\}_2(\mu\text{-N}_2\text{H})]^+$  (B) so that it never attains a sufficiently high concentration to be detected spectrophotometrically.

One final feature is worth noting in the context of these studies and that related to the application of the steady-state treatment to the species (B). Such a treatment assumes that under all the conditions studied,  $k_2[\text{HCl}] > k_{-1}[\text{Cl}^-]$ . Inspec-

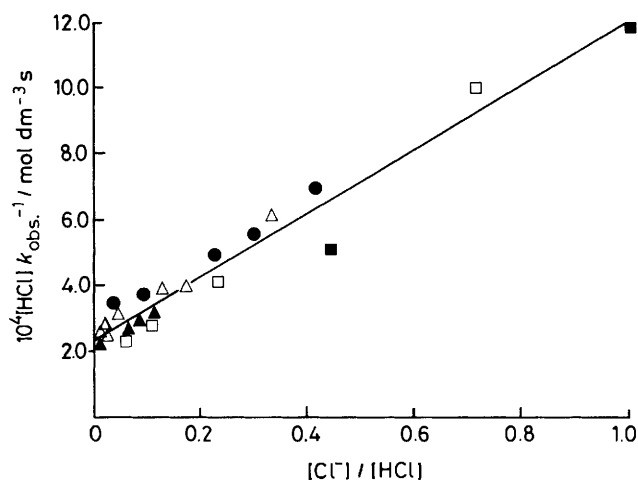


**Figure 3.** Graph of  $[\text{HCl}]/k_{\text{obs.}}$  against  $[\text{Cl}^-]/[\text{HCl}]$  for the reaction between  $[\{\text{Ta}(\text{S}_2\text{CNEt}_2)_3\}_2(\mu\text{-N}_2)]$  and HCl in the presence of [NEt<sub>4</sub>]Cl in MeCN at  $25.0^\circ\text{C}$ . Data points shown: [HCl] = 2.0, [Cl<sup>-</sup>] = 1.0–4.0 (■); [HCl] = 10.0, [Cl<sup>-</sup>] = 1.0–6.0 (●); [HCl] = 20.0, [Cl<sup>-</sup>] = 1.0–8.0 (▲); [HCl] = 2.5–20.0, [Cl<sup>-</sup>] = 1.0 (Δ); and [HCl] = 5.0–20.0, [Cl<sup>-</sup>] = 4.0 mmol dm<sup>-3</sup> (□)

tion of the data in Table 1 shows that this inequality is always true, thus vindicating the steady-state treatment adopted.

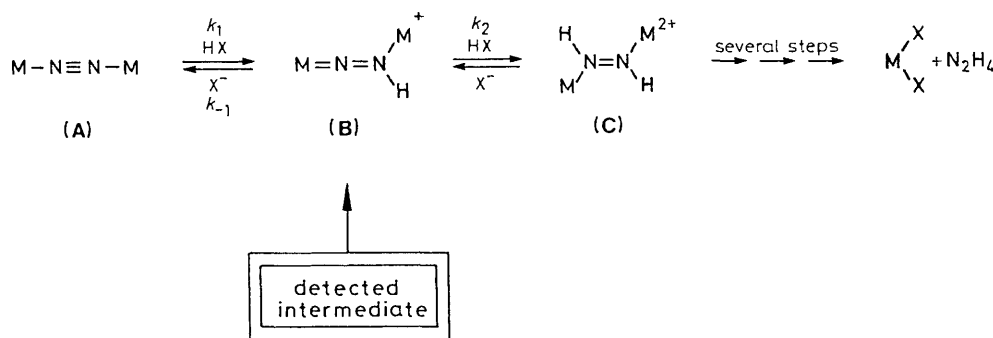
**Reaction of  $[\{\text{Nb}(\text{S}_2\text{CNEt}_2)_3\}_2(\mu\text{-N}_2)]$  with HBr.**—The reaction of  $[\{\text{Nb}(\text{S}_2\text{CNEt}_2)_3\}_2(\mu\text{-N}_2)]$  with an excess of HBr exhibits a single, exponential absorbance-time trace and no intermediates could be detected in this system. The kinetics of the reaction exhibited a first-order dependence on the concentration of dinitrogen complex, but a complicated dependence on the concentration of HBr as shown by the data in Table 2 and illustrated in Figure 5 (insert). Before analysing these data it is informative to understand the kinetics of this system in the presence of [NBu<sup>n</sup>]<sub>4</sub>Br.

In the presence of an excess of both HBr and [NBu<sup>n</sup>]<sub>4</sub>Br the kinetics of the reaction with  $[\{\text{Nb}(\text{S}_2\text{CNEt}_2)_3\}_2(\mu\text{-N}_2)]$  exhibits a first-order dependence on the concentration of dinitrogen complex but a complicated dependence on the concentrations of acid and bromide as shown in Figure 5 and described by equation (7). Kinetic data for the studies of the niobium

$$k_{\text{obs.}} = \frac{(2.4 \pm 0.2) \times 10^2 [\text{HBr}]^2}{[\text{Br}^-] + (0.080 \pm 0.01)[\text{HBr}]} \quad (7)$$

complex are shown in Table 2. Here, as before, the concentrations of HBr and Br<sup>-</sup> have been calculated using the literature values<sup>6</sup> for the homoconjugation equilibrium constant ( $K_{\text{Br}} = 2.51 \times 10^2 \text{ dm}^3 \text{ mol}^{-1}$ ) and acid-base equilibrium constant ( $K_{\text{a}} = 3.16 \times 10^{-6}$ ) for HBr corresponding to equations (3) and (4). Equation (7) is identical, in form, to (5) and (6), and comparison with (6) permits the determination of  $k_1 = (3.0 \pm 0.1) \times 10^3 \text{ dm}^3 \text{ mol}^{-1} \text{ s}^{-1}$  and  $k_2/k_{-1} = 0.080 \pm 0.01$ . Unfortunately, in this case, we do not have an independent means of determining the value of  $k_2$ .

Using the values of  $k_1$  and  $k_2/k_{-1}$  obtained from the studies in the presence of [NBu<sup>n</sup>]<sub>4</sub>Br, and calculating the concentrations of HBr and Br<sup>-</sup> for the original studies where no [NBu<sup>n</sup>]<sub>4</sub>Br was added, then the dependence on the concentration of HBr can be predicted as shown by the curve in Figure 5 (insert). Although the fit to the data is very good, it is not exact. In particular, the fit tends to overestimate the values of  $k_{\text{obs.}}$  particularly at low concentrations of HBr. This may be a consequence of the literature value used for  $K_{\text{Br}}$  (determined



**Scheme.** Mechanism for the reaction between  $[\{\text{M}(\text{S}_2\text{CNET}_2)_3\}_2(\mu\text{-N}_2)]$  ( $\text{M} = \text{Nb}$  or  $\text{Ta}$ ) and acid in MeCN. Dithiocarbamato-ligands omitted for clarity

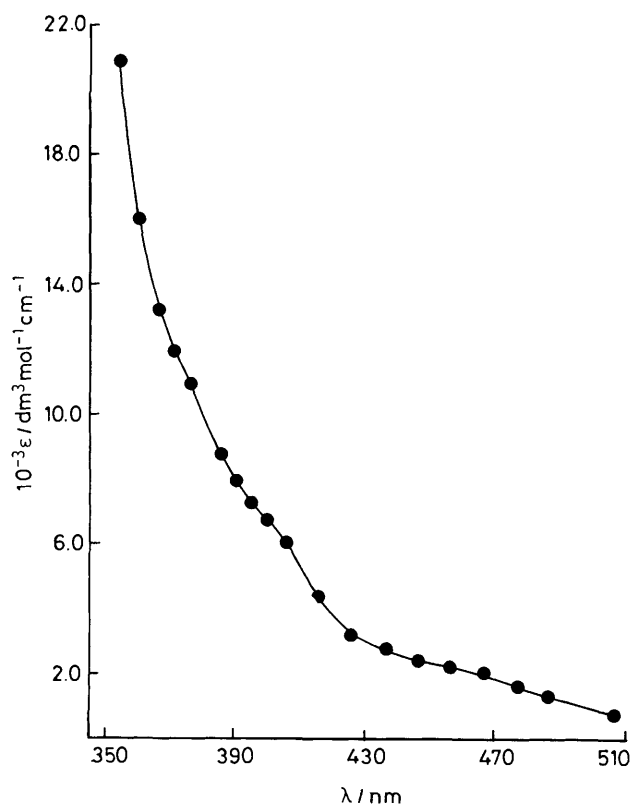


**Figure 4.** Visible absorption spectrum of  $[\{\text{Ta}(\text{S}_2\text{CNET}_2)_3\}_2(\mu\text{-N}_2\text{H})]^+$  detected in the reaction of  $[\{\text{Ta}(\text{S}_2\text{CNET}_2)_3\}_2(\mu\text{-N}_2)]$  with HCl in MeCN

using the  $[\text{NEt}_4]^+$  salt.<sup>6</sup> It may be that the nature of the cation has an effect on the value of this homoconjugation equilibrium constant.

**Reaction of  $[\{\text{Nb}(\text{S}_2\text{CNET}_2)_3\}_2(\mu\text{-N}_2)]$  and HCl.**—The reaction between  $[\{\text{Nb}(\text{S}_2\text{CNET}_2)_3\}_2(\mu\text{-N}_2)]$  and an excess of HCl in MeCN occurs with a single exponential absorbance-time trace ( $\lambda = 370 \text{ nm}$ ). The rate of the reaction exhibits a first-order dependence on the concentration of dinitrogen complex and a first-order dependence on the acid concentration over the range studied,  $5.0 < [\text{HCl}] < 50.0 \text{ mmol dm}^{-3}$ . The kinetic data are collected in Table 2, and the rate equation is given by (2), where  $a = 0.62 \pm 0.05 \text{ dm}^3 \text{ mol}^{-1} \text{ s}^{-1}$ . This rate equation is consistent with the expression (6), if  $k_2[\text{HCl}] \gg k_{-1}[\text{Cl}^-]$ , in which case the limiting form of equation (6) is that shown in (8).

$$k_{\text{obs.}} = k_1[\text{HCl}] \quad (8)$$

**Table 2.** Kinetic data for the reactions of  $[\{\text{Nb}(\text{S}_2\text{CNET}_2)_3\}_2(\mu\text{-N}_2)]$  ( $2.5 \times 10^{-5} \text{ mol dm}^{-3}$ ) with HCl or HBr in MeCN ( $25.0^\circ\text{C}$ ,  $\lambda = 370 \text{ (Cl)}$  or  $420 \text{ nm (Br)}$ )

X	$[\text{HX}]^a / \text{mmol dm}^{-3}$	$[\text{X}^-]^{a,b} / \text{mmol dm}^{-3}$	$k_{\text{obs.}}^c / \text{s}^{-1}$	
Cl <sup>d</sup>	5.0		$1.8 \times 10^{-3}$	
	6.5		$4.0 \times 10^{-3}$	
	12.5		$7.8 \times 10^{-3}$	
	18.2		$12.4 \times 10^{-3}$	
	23.5		$13.8 \times 10^{-3}$	
	28.6		$17.2 \times 10^{-3}$	
	33.3		$18.3 \times 10^{-3}$	
	37.8		$23.0 \times 10^{-3}$	
Br	2.0		1.2	
	3.0		3.7	
	5.0		10.5	
	5.0 <sup>e</sup>		10.2	
	5.0 <sup>f</sup>		11.6	
	6.0		15.8	
	8.0		25.0	
	10.0		25.7	
	12.5		38.3	
	15.0		50.0	
	17.5		43.5	
	20.0		50.0	
	Br	5.0	0.5	9.2(5.0)
			1.0	4.9(3.2)
			2.0	2.5(2.1)
		5.0	0.42(0.42)	
		10.0	0.16	
10.0		0.5	22.0(11.0)	
		1.0	26.0(11.3)	
		2.0	14.5(7.0)	
		5.0	5.2	
20.0		0.5	44.1(21.8)	
		1.0	48.0(27.0)	
	2.0	42.2(20.5)		
	5.0	25.0(17.3)		
	10.0	(6.8)		

<sup>a</sup> Concentrations of HX and  $\text{X}^-$  shown are those added to the reaction mixture. The concentrations shown in the Figures are those corrected for the corresponding homoconjugation and acid-base equilibria.

<sup>b</sup> Bromide supplied as  $[\text{NBu}_4]\text{Br}$ . <sup>c</sup> Values shown in parentheses are the rate constants measured using DBr. <sup>d</sup>  $7.2 \times 10^{-5} \text{ mol dm}^{-3}$   $[\{\text{Nb}(\text{S}_2\text{CNET}_2)_3\}_2(\mu\text{-N}_2)]$ . <sup>e</sup>  $1.6 \times 10^{-5} \text{ mol dm}^{-3}$   $[\{\text{Nb}(\text{S}_2\text{CNET}_2)_3\}_2(\mu\text{-N}_2)]$ . <sup>f</sup>  $3.2 \times 10^{-5} \text{ mol dm}^{-3}$   $[\{\text{Nb}(\text{S}_2\text{CNET}_2)_3\}_2(\mu\text{-N}_2)]$ .

**The Rates and Sites of Proton Transfer to Bridging Dinitrogen Ligands.**—In the three studies described herein the reaction between an acid and  $[\{\text{M}(\text{S}_2\text{CNET}_2)_3\}_2(\mu\text{-N}_2)]$  to form hydrazine according to equation (1) is rate-limited by either the first or second protonation of the dinitrogen residue. The elementary rate constants measured in all these systems and the

**Table 3.** Summary of elementary rate constants and primary isotope effects in the reactions of acid with  $[\{M(S_2CNEt_2)_3\}_2(\mu-N_2)]$  ( $M = Nb$  or  $Ta$ )

Metal	Acid	$k_1/\text{dm}^3 \text{ mol}^{-1} \text{ s}^{-1}$	$k_2/\text{dm}^3 \text{ mol}^{-1} \text{ s}^{-1}$	$k_2/k_{-1}$	Comments and isotope effects
Ta	HCl	$(4.5 \pm 0.1) \times 10^3$	$(1.3 \pm 0.1) \times 10^4$	$0.25 \pm 0.02$	$k_{-1} = (5.2 \pm 0.1) \times 10^4 \text{ dm}^3 \text{ mol}^{-1} \text{ s}^{-1}$ $k_1^H/k_1^D = 1.25$ $k_2^H/k_2^D = 1.37$
Nb	HCl	$0.62 \pm 0.05$			
Nb	HBr	$(3.0 \pm 0.1) \times 10^3$		$0.08 \pm 0.01$	$k_1^H/k_1^D = 1.97$ $(k_2^H/k_2^D)/(k_1^H/k_1^D) = 0.67$

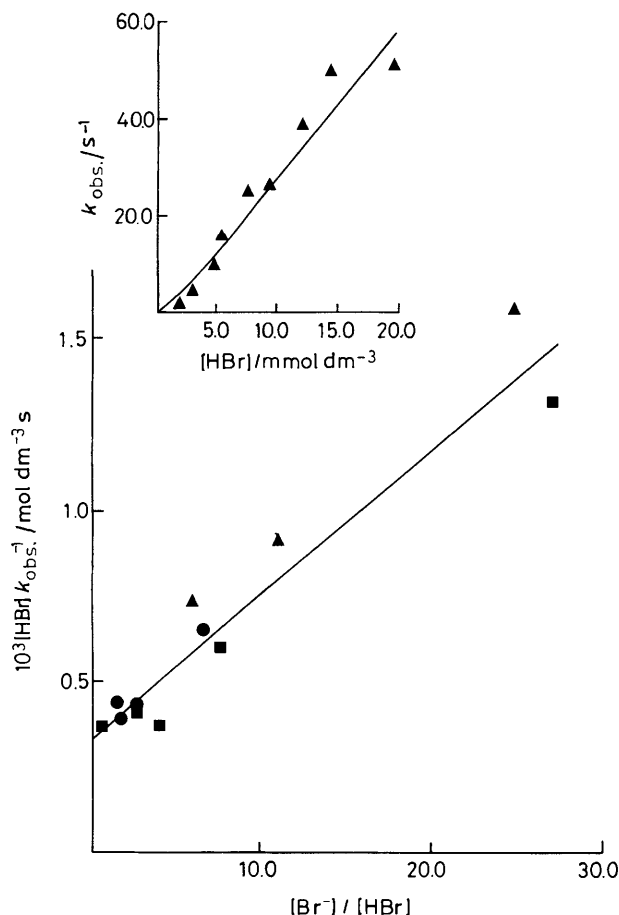


**Figure 5.** Graph of  $[HBr]/k_{obs.}$  against  $[Br^-]/[HBr]$  for the reaction between  $[\{Nb(S_2CNEt_2)_3\}_2(\mu-N_2)]$  and HBr in the presence of  $[NBu_4]Br$  in MeCN at 25.0 °C. Data points shown:  $[HBr] = 5.0$ ,  $[Br^-] = 0.5-10.0$  ( $\blacktriangle$ );  $[HBr] = 10.0$ ,  $[Br^-] = 0.5-5.0$  ( $\blacksquare$ ); and  $[HBr] = 20.0$ ,  $[Br^-] = 0.5-5.0$  mmol  $\text{dm}^{-3}$  ( $\bullet$ ). Insert: graph of  $k_{obs.}$  against the concentration of HBr. Curve drawn is that predicted by equation (7)

primary isotope effects associated with the proton-transfer reactions are collected in Table 3.

Several features of these collected rate constants are worthy of further discussion. In particular the influence of the metal on the rate of proton transfer to the dinitrogen residue can be compared in the two studies with HCl, where  $k_1^{Ta}/k_1^{Nb} = 6.9 \times 10^3$ . The greater reactivity of the complex containing the third-row metal towards protonation has been observed in the reactions of mononuclear complexes containing end-on coordinated dinitrogen molecules<sup>7,10</sup> such as, *trans*- $[M(N_2)_2(L-L)_2]$  ( $M = Mo$  or  $W$ ,  $L-L =$  chelating ditertiary diphosphine). This reactivity trend is a consequence of the more electron-releasing nature of the heavier element,<sup>11</sup> which increases the basicity of the dinitrogen ligand. This effect

has one further consequence in the studies on the bridging dinitrogen complexes described herein. The acidity of  $[\{Ta(S_2CNEt_2)_3\}_2(\mu-N_2H)]^+$  (**B**) is so low in the HCl system that it attains a sufficient concentration to be detected. In contrast, with the less electron-releasing niobium system, the high acidity of  $[\{Nb(S_2CNEt_2)_3\}_2(\mu-N_2H)]^+$  precludes its spectrophotometric detection, and its presence can only be implied from the kinetics.

The influence of the acid on the rate of proton transfer to the bridging dinitrogen ligand can be judged from the studies with  $[\{Nb(S_2CNEt_2)_3\}_2(\mu-N_2)]$  where  $k_1^{HBr}/k_1^{HCl} = 4.8 \times 10^3$ . This difference in reactivity for the reactions with the two acids correlates well with their acid strength in MeCN,<sup>6</sup>  $K_a^{HBr}/K_a^{HCl} = 2.5 \times 10^3$ , and is a reactivity pattern which has also been observed for mononuclear dinitrogen complexes.

The crucial difference between bridging dinitrogen complexes and mononuclear dinitrogen complexes lies in the rates of proton transfer to the nitrogenous residue. The proton-transfer rate constants to the bridging dinitrogen ligand in  $[\{M(S_2CNEt_2)_3\}_2(\mu-N_2)]$  are relatively low (Table 3), whereas the corresponding rate constants for the protonation of mononuclear dinitrogen ligands in *trans*- $[M(N_2)_2(L-L)_2]$  have been estimated to be  $k \geq 4 \times 10^6 \text{ mol}^{-1} \text{ s}^{-1}$ , and are probably diffusion-controlled.<sup>12</sup> The origin of this difference in reactivity resides, at least in part, in the availability of a lone pair of electrons on the remote nitrogen atom of mononuclear dinitrogen complexes. Protonation at this lone pair can result in rapid rates of protonation for thermodynamically favourable reactions. In binuclear systems no such lone pair is available, and thus protic attack at a bridging dinitrogen residue must involve a higher-energy interaction of the acid with the delocalised electron density of the bridging unit.

In the Scheme we have proposed, like others before,<sup>2,3,13</sup> that the site of the second protonation is the unprotonated nitrogen atom, to give a diazene species,  $[\{M(S_2CNEt_2)_3\}_2(\mu-NH-NH)]^{2+}$  (**C**). However we cannot convincingly dismiss the other possibility, namely  $[\{M(S_2CNEt_2)_3\}_2(\mu-NNH_2)]^{2+}$ . The solution to this dichotomy can only be resolved by isolation and structural characterisation of this species (impossible in the present system because of the rapidity of the subsequent, hydrazine-forming reactions), or the design of a heterobinuclear system which cleaves after diprotonation to give kinetically inert products and the identification of these cleavage products.

It has been argued,<sup>3,13</sup> without any firm experimental evidence, that two metals bound to dinitrogen can impart a greater basicity to the dinitrogen than a single metal, and that during the transformation to ammonia or hydrazine each metal has to supply relatively fewer electrons than a mononuclear system. These claimed advantages of a nitrogen-fixing cycle based on a polynuclear dinitrogen-binding site must be balanced against the kinetic and thermodynamic disadvantages of forming and breaking more than one metal-nitrogen bond during the catalytic cycle. Furthermore, we have shown in this study that the rates of proton transfer from acid to dinitrogen ligand can be much faster for mononuclear systems than in

bridging dinitrogen complexes: another kinetic advantage for mononuclear, end-on co-ordinated dinitrogen complexes.

### Acknowledgements

We thank Miss Kay Oglieve and Mr Ferdia O'Flaherty for skilled technical assistance.

### References

- 1 Part 4, R. A. Henderson, D. L. Hughes, and A. N. Stephens, preceding paper.
- 2 R. A. Henderson, G. J. Leigh, and C. J. Pickett, *Adv. Inorg. Radiochem.*, 1983, **27**, 197 and refs. therein.
- 3 A. E. Shilov, M. E. Vol'pin, and V. B. Shur, 'New Trends in the Chemistry of Nitrogen Fixation,' eds. J. Chatt, L. M. da Câmara Pina, and R. L. Richards, Academic Press, London, 1980, pp. 67 and 121 and refs. therein.
- 4 R. D. Sanner, J. M. Manriquez, R. E. Marsh, and J. E. Bercaw, *J. Am. Chem. Soc.*, 1976, **98**, 8352.
- 5 J. R. Dilworth, R. A. Henderson, A. Hills, D. L. Hughes, C. Macdonald, A. N. Stephens, and D. R. M. Walton, *J. Chem. Soc., Dalton Trans.*, 1990, 1077.
- 6 J. F. Coetzee, *Prog. Phys. Org. Chem.*, 1967, **4**, 45.
- 7 R. A. Henderson, *J. Chem. Soc., Dalton Trans.*, 1982, 917.
- 8 R. A. Henderson and K. E. Oglieve, *J. Chem. Soc., Dalton Trans.*, 1990, 1093.
- 9 J. H. Espenson, 'Chemical Kinetics and Reaction Mechanisms,' McGraw-Hill, New York, 1981, p. 69.
- 10 R. A. Henderson, *J. Organomet. Chem.*, 1981, **208**, C51.
- 11 D. F. Shriver, *Acc. Chem. Res.*, 1970, **3**, 231.
- 12 J. D. Lane and R. A. Henderson, *J. Chem. Soc., Dalton Trans.*, 1987, 197 and refs. therein.
- 13 A. E. Shilov, 'Nitrogen Fixation: Hundred Years After,' eds. H. Bothe, F. J. de Bruijn, and W. E. Newton, Gustav Fischer, Stuttgart, New York, 1988, p. 57.

Received 12th May 1989; Paper 9/01992H